24F04

Effects of Laser Spatial Profile on Fast Electron Generation
レーザーの空間プロファイルが高速電子生成に及ぼす影響

Masayasu Hata, Hitoshi Sakagami[1], Tomoyuki Johzaki[2] and Hideo Nagatomo[3]
畑　昌育, 坂上仁志，城崎知至，長友英夫

Department of Physics, Nagoya University, Furo-cho, Chikusa-ku, Nagoya 464-8602, Japan
名古屋大学大学院理学研究科　〒464-8602　名古屋市千種区不老町
[1]Fundamental Physics Simulation Research Division, National Institute for Fusion Science, Oroshi-cho, Toki 509-5292, Japan
核融合科学研究所基礎物理シミュレーション研究系　〒509-5292　土岐市下石町
[2]Institute of Laser Technology, Yamadaoka, Suita 565-0871, Japan
レーザー技術総合研究所　〒565-0871　吹田市山田丘
[3]Institute of Laser Engineering, Osaka University, Yamadaoka, Suita 565-0871, Japan
大阪大学レーザーエネルギー学研究センター　〒565-0871　吹田市山田丘

2D PIC simulations for fast ignition with a planar target and 200 fs ultrahigh intense laser have been performed to investigate effects of laser spatial profile on fast electron generation. Two cases of different laser spatial profiles, namely Gaussian and super Gaussian are compared, assuming that total energies, temporal profiles, and FWHMs of transverse intensity profile for both lasers are the same. High-energy electrons (> 5 MeV) are much generated near the laser axis and angle divergence is large at the area far from the laser axis in the super Gaussian case compared to the Gaussian case.

1. Introduction

In 1994, fast ignition scheme was proposed [1]. Many studies have intensively been performed since this proposal [2,3]. In Japan, the FIREX-I project [4], of which purpose is the achievement of heating a core up to 5 keV, has been started. Cone-guided targets are used in this project and the design optimization of the target has been being performed [5-7]. In contrast, the laser profile is not optimized so much and its effects on fast electron characteristics are not clarified yet. Therefore, it is necessary for full optimization to investigate effects of laser temporal and spatial profiles. In this paper, we paid attention to laser spatial profiles and estimated those effects on fast electron generation.

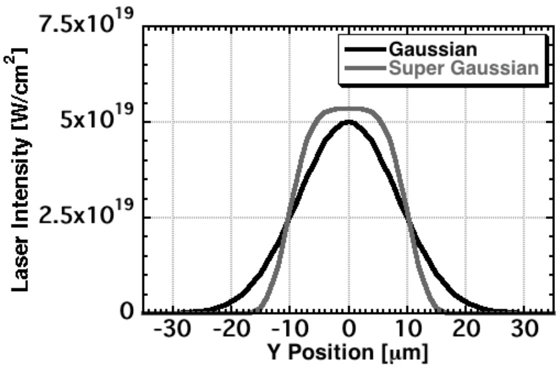

Fig.1. Spatial pulse shape of laser in y direction

2. Simulation Conditions

Laser-plasma interactions on normal incidence of an ultrahigh intense laser to a gold planar target are simulated for 200 fs with 2D PIC code, FISCOF2. We compared two cases of different spatial pulse shapes, namely Gaussian with peak intensity of 5×10^{19} W cm^{-2} and super Gaussian ($\alpha = 4$) of 5.36×10^{19} W cm^{-2} as shown in Fig. 1. Each laser has same total energy, flat temporal profile ($\tau_{flat} = \infty$), and FWHM (full width half maximum) of transverse intensity profile (20 μm). The target is made of the gold with the atomic number of 197, the charge state of 40, and the ion-to-electron mass ratio of 1836. The initial temperatures of electrons and ions are 10 and 1 keV, respectively. The target consists of a preplasma, whose electron density profile is exponential from 0.1 to 20 times critical density (n_{cr}) with the scale length of 4 μm, and a main plasma that has flat electron density profile with the length of 15 μm. The density profile in y direction is uniform and its width is 70 μm. To neglect the circulation of fast electrons, we introduce an artificial cooling region from three edges of the plasma, except the surface of the laser irradiation, to a 6 μm inner side. In this region fast electrons are gradually cooled down to the initial temperature. We observe electrons in the main plasma, 5 μm behind the boundary between pre- and main plasmas in x direction at y = 0–5 and 20–25 μm.

3. Electron Beam Intensity

Figure 2 shows time evolutions of electron beam intensity in the cases of Gaussian and super Gaussian at y = 0–5 and 20–25 μm. At y = 0–5 μm, the electron beam intensity in the super Gaussian case exceeds that of the Gaussian case because the laser intensity of the super Gaussian case at this region is higher than that of the Gaussian case as shown in Fig. 1. On the other hand, the electron beam intensity at y = 20–25 μm in the super Gaussian case is lower than that of the Gaussian case as the laser in the super Gaussian case is less intense than that of the Gaussian case at the area far from the laser axis.

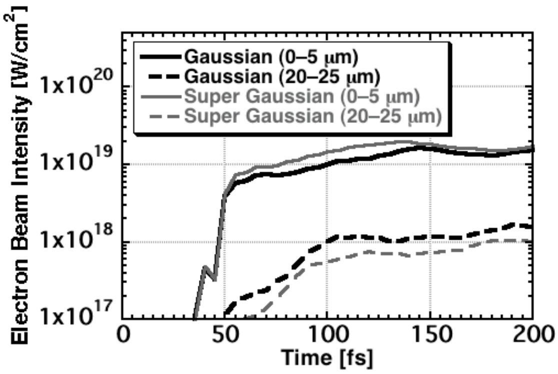

Fig.2. Time evolutions of electron beam intensity

4. Time-integrated electron energy spectra

In fast ignition, the electron energy distribution is extremely significant because the stopping distance of the electron in the core varies with its energy. Figure 3 shows time-integrated energy spectra of electrons in the cases of Gaussian and super Gaussian at y = 0–5 and 20–25 μm. Near the laser axis, high-energy (> 5 MeV) fast electrons in the case of super Gaussian are more generated than that of the Gaussian case as the laser intensity of the super Gaussian case is higher than that of the Gaussian case, but the number of low-energy electrons is similar. In contrast, at the area far from the laser axis, low-energy (< 3 MeV) electrons in the super Gaussian case are less generated than that of Gaussian because the laser of super Gaussian is less intense than that of Gaussian.

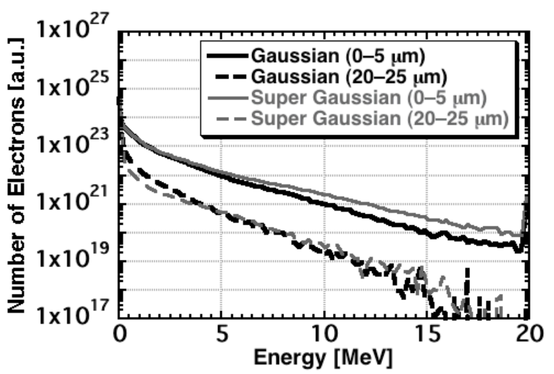

Fig.3. Time-integrated electron energy spectra

5. Divergence angle of electrons

It is important for efficient core heating to investigate divergence angle of fast electrons. Figure 4 shows HWHMs of angle as a function of electron energy on electron momentum distribution at y = 0–5 and 20–25 μm. Near the laser axis, HWHMs in both cases are similar. On the other hand, HWHMs in the super Gaussian case are larger than those of the Gaussian case at the area far from the laser axis. In the super Gaussian case, most of the observed electrons are generated not at the outer region but at the area close to the laser axis, as the outside laser intensity is so low compared to the Gaussian case. Therefore, at the outer region, electron divergence becomes large in the super Gaussian case.

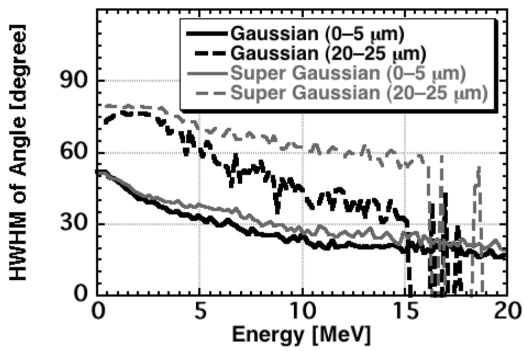

Fig.4. HWHMs of angle as a function of electron energy on electron momentum distribution

References

[1] M. Tabak, J. Hammer, M.E. Glinsky, W.L. Kruer, S.C. Wilks, E.M. Gampbell et al.: Phys. Plasmas **1** (1994) 1626.

[2] M. Tabak, D. Clark, S. Hatchett, M. Key, B. Lasinski, R. Snavely et al.: Phys. Plasmas **12** (2005) 057305.

[3] P. Norreys, R. Scott, K. Lancaster, J. Green, A. Robinson, M. Sherlock et al.: Nuclear Fusion **49** (2009) 104023.

[4] H. Azechi and The FIREX Project.: Plasma Phys. Control. Fusion **48** (2006) B267.

[5] H. Sakagami, T. Johzaki, H. Nagatomo and K. Mima: Nuclear Fusion **49** (2009) 075026

[6] H. Nagatomo, T. Johzaki, H. Sakagami, Y. Sentoku, A. Sunahara, T. Taguchi, H. Shiraga, H. Azechi and K. Mima: Nuclear Fusion **49** (2009) 075028

[7] T. Johzaki, H. Nagatomo, A. Sunahara, H.-B. Cai, H. Sakagami, Y. Nakao and K. Mima: Nuclear Fusion **51** (2011) 073022